Influence of subglacial geology on the onset of a West Antarctic ice stream from aerogeophysical observations

R. E. Bell*, D. D. Blankenship†, C. A. Finn‡, D. L. Morse†,
T. A. Scambos§, J. M. Brozena‖ & S. M. Hodge¶

* Lamont-Doherty Earth Observatory of Columbia University, Palisades,
New York 10964, USA
† Institute for Geophysics, University of Texas at Austin, Austin, Texas 78759, USA
‡ US Geologic Survey, Denver, Colorado 80225, USA
§ National Snow and Ice Data Center, Boulder, Colorado 80309, USA
‖ Naval Research Laboratory, Washington DC 20375, USA
¶ US Geologic Survey, Tacoma, Washington 98406, USA

....

**Marine ice-sheet collapse can contribute to rapid sea-level rise[1].
Today, the West Antarctic Ice Sheet contains an amount of ice
equivalent to approximately six metres of sea-level rise, but most
of the ice is in the slowly moving interior reservoir. A relatively
small fraction of the ice sheet comprises several rapidly flowing ice
streams which drain the ice to the sea. The evolution of this
drainage system almost certainly governs the process of ice-sheet
collapse[2–5]. The thick and slow-moving interior ice reservoir is
generally fixed to the underlying bedrock while the ice streams
glide over lubricated beds at velocities of up to several hundred
metres per year. The source of the basal lubricant—a water-
saturated till[6,7] overlain by a water system[8]—may be linked to
the underlying geology. The West Antarctic Ice Sheet rests over a
geologically complex region characterized by thin crust, high heat
flows, active volcanism and sedimentary basins[9–16]. Here we use
aerogeophysical measurements to constrain the geological setting
of the onset of an active West Antarctic ice stream. The onset
coincides with a sediment-filled basin incised by a steep-sided
valley. This observation supports the suggestion[5,17] that ice-stream
dynamics—and therefore the response of the West Antarctice Ice
Sheet to changes in climate—are strongly modulated by the
underlying geology.**

We use satellite imagery to identify streaming ice in central West
Antarctica[18] (Fig. 1). The 20-km-wide region, with distinct margins
bordering featureless ice (Fig. 2a), is dominated by flow-parallel
banding and surface undulations, characteristic of streaming ice[19,20].
Streaming has been confirmed by GPS (Global Positioning System)
measurements of surface ice velocity along a seismic line crossing
the southern margin (Fig. 2c)[21]. New aerogeophysical data support
the ice-streaming identification. Airborne ice-penetrating radar
profiles show disrupted internal layering between the identified
margins (Fig. 3). In the satellite image, the flow-parallel bands begin
downslope (west) of a prominent, dark 'S'-shaped feature. Airborne
laser altimetry (Fig. 2b) shows that this 'S' is caused by a 100-m-high
escarpment in the ice surface which marks a significant break in ice
surface slope. Upstream (east) of the 'S', the ice surface has a mean
slope over 25 km of 7 m km^{-1} which decreases to 3 m km^{-1} down-
stream. The corresponding driving stress for ice-sheet flow
decreases from over 100 kPa upstream of the 'S' to 60 kPa down-
stream. We interpret the 'S' as the onset of streaming, and will refer
to the portion of the ice stream downstream of this 'S' as the onset
region.

Ice-penetrating radar data (Fig. 2d) shows that the onset of
streaming rests over low-lying southwest-dipping subglacial topo-
graphy. The onset 'S' is bounded by a plateau to the north and a
prominent ridge to the south. Two kilometres west (downstream) of
the 'S', the ice stream flows in a subglacial valley bounded by steep

walls (10° or greater) (Fig. 4a). This valley has a maximum depth of
~1,900 m below sea level which shallows to 1,300 m below sea level
at the western edge of the survey area. Both the aeromagnetic and
airborne gravity data reveal contrasting geological structures
beneath the onset region. An elongate east–west-orientated 50 nT
magnetic low is centred over the region (Fig. 2f) coincident with an
elongate east–west-orientated free-air gravity low (Fig. 2e). The
gravity low is ~25 km across, with amplitudes as large as 50 mGal
below the regional value. These anomalies appear to outline the ice-
stream margins identified by satellite imagery (Fig. 4b). A seismic
profile (Fig. 2c) shows that the southern boundary of the ice stream,
10 km to the west of the aerogeophysical study area, is coincident
with low-velocity material interpreted as a sedimentary basin[21].

We hypothesize that geological structures control the position of
both the ice-stream margins and onset; this can be tested with
potential field models. To constrain the geological structures, we
constructed a model of the magnetic and gravity anomalies along a
profile perpendicular to the ice stream downstream of the onset 'S'
(profile B, Fig. 2). The simplest model which fits the potential
field data consists of three bodies interpreted as three geological
units (Fig. 4c). The density (2,690 kg m^{-3}) and magnetization
(3.8 A m^{-1}) of the prominent basement ridge south of the ice
stream are equivalent to gabbros or highly compacted basalt
flows. North of 30 km along profile B, the basement (or lower
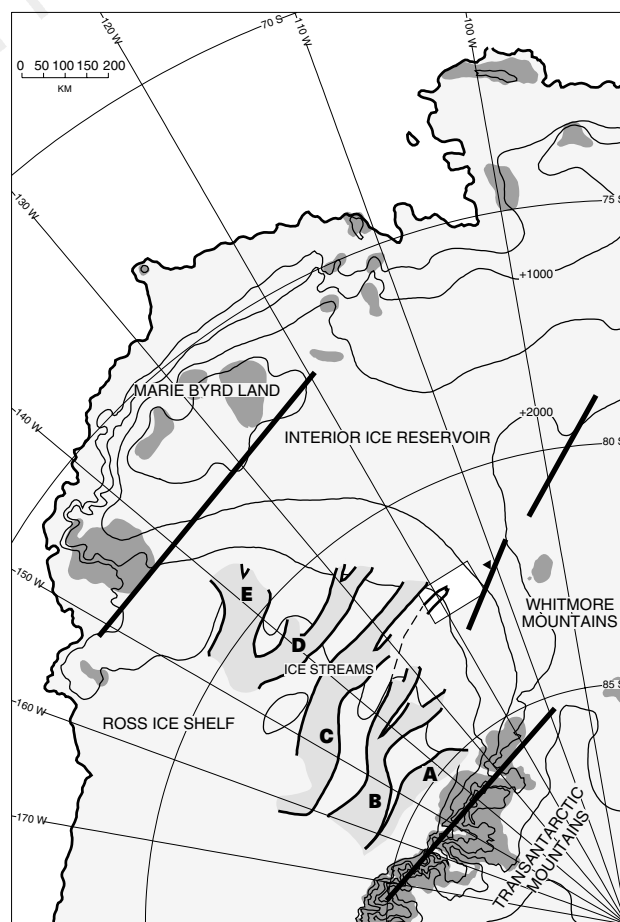geological unit) is characterized by material of lower density

Figure 1 Map of the West Antarctic Ice Sheet. 500-m surface elevation contours
are shown[23]. The intermediate shading indicates the ice streams[24]. The white box
is the location of the satellite image (Fig. 2). The onset region studied here (bold
outline within the white box) and its proposed flow boundaries (dashed) are
shown. The onset region is connected to Ice Stream B as suggested by a recent
water piracy hypothesis[25]. Heavy lines delineate the approximate flanks of the
West Antarctic rift system, and the small triangle locates an active volcano[5].

(2,500 kg m^{-3}) and magnetization (1.3 A m^{-1}); this material may possibly be interlayered volcanic flows and sediments or volcaniclastic sediments. A geological model which contains only these two basement units does not adequately match the observed gravity and magnetic anomalies (r.m.s. residuals of 8.0 mGal and 15 nT for gravity and magnetics, respectively): a third geological unit is necessary to match the observed anomalies.

This third unit is constrained to correspond to sedimentary rocks by the seismic observation of 600–1,500 m of low-velocity material beneath the ice stream 20 km to the west[21]. Assignment of a geologically reasonable but low density (2,130 kg m^{-3}) and zero magnetization to the unit resulted in an average thickness of 1,000 m of sedimentary rocks extending from 11 km to 35 km along profile B. Although the densities and magnetizations are poorly constrained, this model shows the minimum thickness of low-density material necessary to match the potential field observations (r.m.s. residuals are 2.9 mGal for the gravity and 13 nT for the magnetics). The possible sediment thickness ranges from 1,000 to 2,400 m, using the range of geologically reasonable densities (2,130–2,400 kg m^{-3}). The lateral boundaries of the sedimentary basin are constrained by this modelling to within ±1.5 km.

The modelling of profile B strongly suggests that the lateral boundaries of the ice stream near the onset of streaming are coincident with the margins of a sedimentary basin. Sedimentary basins are often long, linear features bounded by elevated topography on one or both sides. From the seismic line and the modelling along profile B we interpret this sedimentary basin as being an elongate feature orientated east–west, roughly coincident with the ice-stream margins. The unique potential field signature of this sedimentary basin is the coincident gravity and magnetic lows whose edges approximately delimit the lateral boundaries of the basin. This coincidence ceases upslope of the onset 'S' where the gravity and magnetic trends have significantly different orientations (Figs 2 and 4b). The question arises as to whether the sedimentary basin—which beneath the onset region contains a minimum of
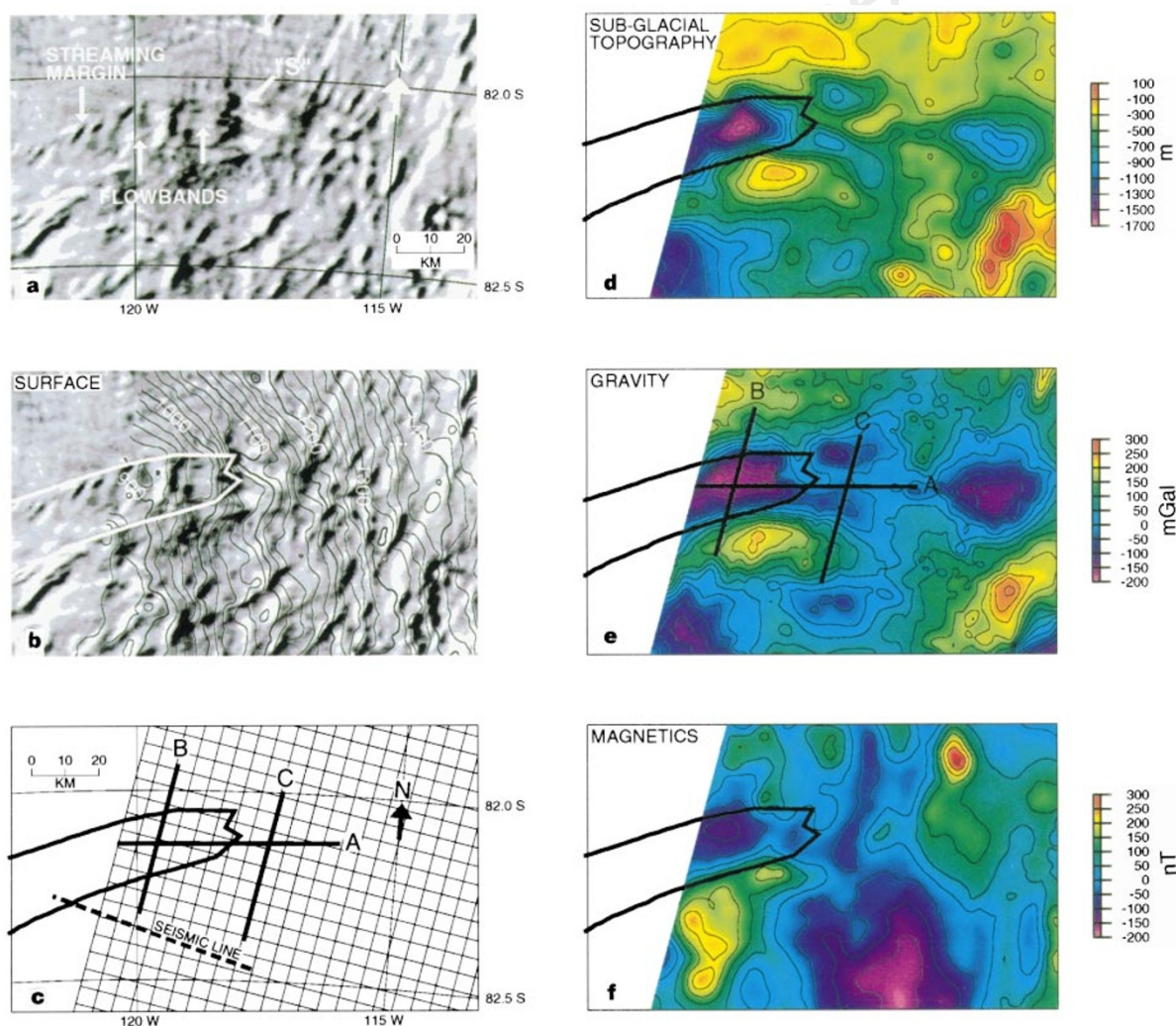

Figure 2 Aerogeophysical maps and satellite images of the onset region. See ref. 5 for a description of the acquisition of these data. **a**, AVHRR (Advanced Very High Resolution Radiometer) image. The image is 145 × 90 km and is orientated in an approximately east–west direction with illumination from the southeast. **b**, Surface elevation of the onset region from airborne laser altimetry superimposed on AVHRR image. The ice surface elevation was constructed from laser ranges to the ice surface and precise differential carrier phase GPS aircraft positions[26]. The bold white line indicates the ice-stream margins interpreted from the AVHRR imagery. **c**, Location of aerogeophysical tracklines, profile A, profile B, profile C and the seismic line of Anandakrishnan and others[21]. Profiles A, B and C are flightlines. The elevated ice surface velocities (>60 m yr^{-1}; ref. 21) are west of the ice-stream margin interpreted from the AVHRR image. **d**, Subglacial topography map. Constructed from radar ice-thickness measurements and surface elevations from GPS-positioned laser ranges. Contour interval is 100 m. **a**, Free-air gravity map. Contour interval is 5 mGal (ref. 26). The locations of profiles A and B are shown. **f**, Magnetic anomaly map. The aeromagnetic data corrected for diurnal signals and the reference field. Contour interval is 50 nT (ref. 27).
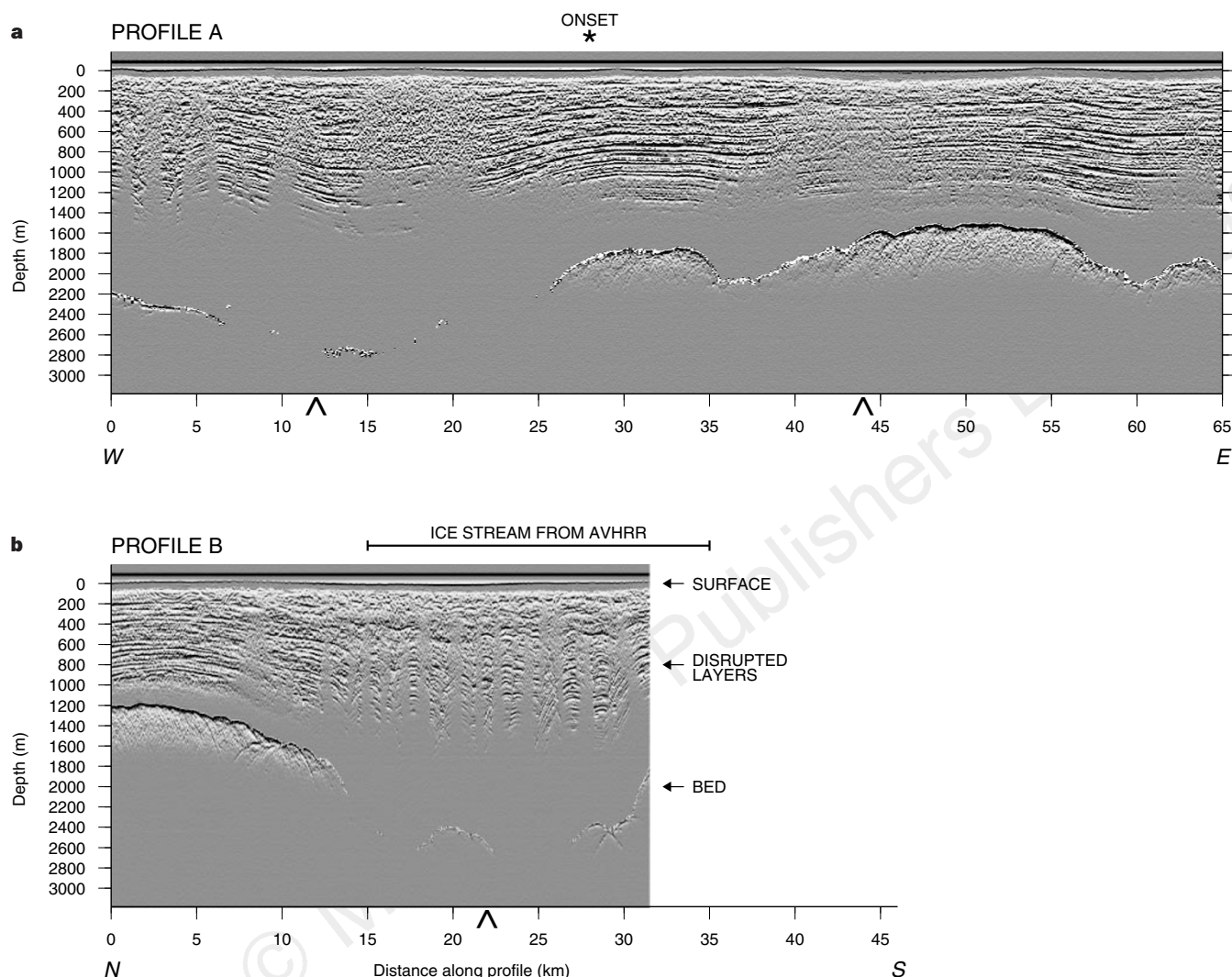
Figure 3 Radar profiles. **a**, Profile A ice-penetrating radar image along ice flow. Ice surface is the uppermost undulating dark band; 1,847 picks of bed position are marked by the lowermost sequence of white pixels. The symbol at 10.6 km indicates the intersection of profile B, and the symbol at 44 km indicates the intersection of profile C. **b**, Profile B ice-penetrating radar image across ice flow including 793 picks of bed position. This particular radar image does not extend the full width of profile B. The symbol at 22 km indicates the intersection of profile A.

1 km of low-density low-magnetism material—terminates close to the onset 'S' as suggested by the diverging gravity and magnetic trends. Construction of a potential field model across the onset region and parallel to the ice flow (profile A in Fig. 2) would be an approach to addressing this question, but the bounding steep topography with variable density makes construction of a simple 2 (or 2.5) dimensional model impracticable. We have modelled a third profile (profile C, Fig. 4d) 10 km upstream of the onset 'S' parallel to profile B. The potential field anomalies along this profile cannot be adequately matched with a sedimentary basin. The gravity anomaly can be matched using the same two-body basement structure used in profile B but without a sedimentary basin, while the magnetic anomaly can be closely matched using a single magnetization for the entire profile, suggesting a change in the magnetic source in the region (r.m.s. residuals are 2.3 mGal for the gravity and 17.5 nT for the magnetics).

We interpret these modelling results as indicating that there is a close correlation between the margins of the ice stream and the sedimentary basin, and that the upstream edge of the sedimentary basin is closely coincident spatially with the onset of streaming. Given that the boundaries of the geological structures are generally coincident with the ice-stream boundaries, we believe that the position of this sedimentary basin controls the position of the ice-stream margins and onset. Thin layers of sediments (10–100 m) cannot be resolved with potential field modelling and may be more widely distributed; but the thicker sequence of sediments found within a sedimentary basin have the potential to focus the streaming process by providing a longer-term source of basal lubricant.

Ice streams have been previously linked to topographic troughs[14] resulting from erosion[22]. This new evidence linking the onset of ice streaming with an underlying sedimentary basin implies that ice streams may only develop over relatively continuous sedimentary basins. Fault-bounded sedimentary basins may be pre-existing topographic troughs but the erosion beneath an ice stream will accentuate any topographic trough, possibly producing erosional unconformities and oversteepened slopes within the scoured sedimentary basin[16]. Furthermore, we suggest the steep slopes of the subglacial valley (over 10°) are too steep to be the result of the initial marine deposition of the sediments within the basin, and may be indicative of active scouring of the sedimentary basin by the ice stream. The erosion of the sedimentary unit beneath the ice stream could provide the fine-grained material necessary to form a lubricating basal till.

This linkage of the onset of an Antarctic ice stream to the underlying geology raises the question of how the complex geology beneath the West Antarctic Ice Sheet may modulate long-term ice-
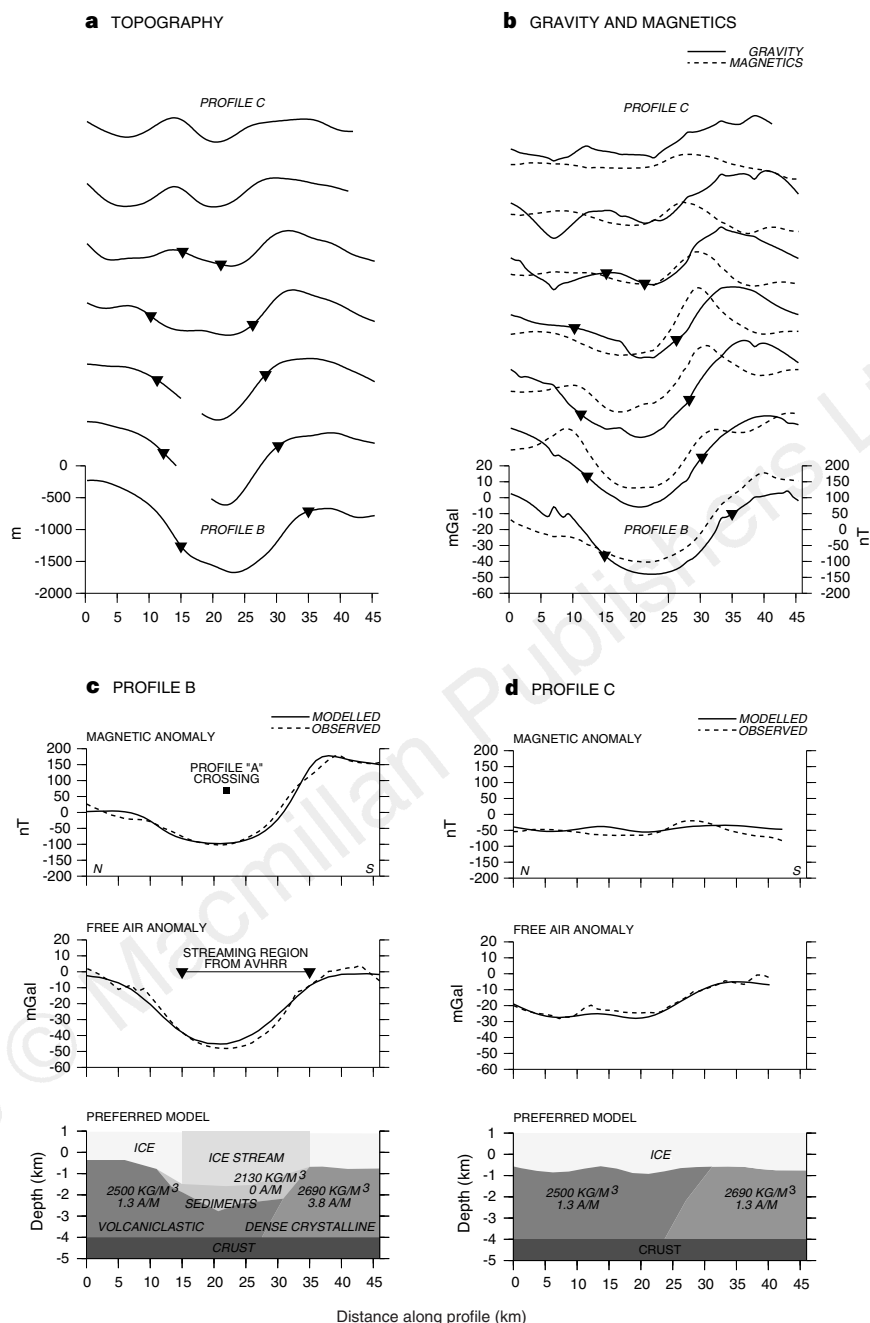
a TOPOGRAPHY

PROFILE C

PROFILE B

b GRAVITY AND MAGNETICS

— *GRAVITY*
--- *MAGNETICS*

PROFILE C

PROFILE B

c PROFILE B

— *MODELLED*
--- *OBSERVED*

MAGNETIC ANOMALY

PROFILE "A" CROSSING

FREE AIR ANOMALY

STREAMING REGION FROM AVHRR

PREFERRED MODEL

ICE   ICE STREAM

2500 KG/M³   2130 KG/M³   2690 KG/M³
1.3 A/M   0 A/M   3.8 A/M
SEDIMENTS

VOLCANICLASTIC   DENSE CRYSTALLINE

CRUST

d PROFILE C

— *MODELLED*
--- *OBSERVED*

MAGNETIC ANOMALY

FREE AIR ANOMALY

PREFERRED MODEL

ICE

2500 KG/M³   2690 KG/M³
1.3 A/M   1.3 A/M

CRUST

Distance along profile (km)

Figure 4 Potential field modelling results and stacked profiles. Ice-stream boundaries (noted with triangles) and onset were determined from the satellite imagery (Fig. 2b). **a**, Stacked subglacial topography profiles every 5.3 km beginning at profile B and extending to profile C. **b**, Stacked free-air gravity (solid lines) and magnetics (dashed lines) anomalies every 5.3 km beginning at profile B and extending to profile C. These profiles show the coincident gravity and magnetics lows which disappear just upstream of the onset. **c**, Potential field model down-

stream of onset 'S'. Shown are profile B observed gravity and magnetic values and calculated values for model with parameters below. Also shown is an illustration of the fault-bounded sedimentary basin model. Ice-stream boundaries were determined from the satellite imagery. **d**, Potential field model upstream of onset 'S'. Shown are profile C observed gravity and magnetic values and calculated values, for the model with parameters shown below.

sheet behaviour driven by global climate oscillations. We suggest that the onset of West Antarctic ice streaming can only develop over sedimentary basins (in the presence of sufficient water). The critical question is whether ice streams can only migrate along sedimentary basins or whether they can develop independently within the present interior ice reservoir. If sedimentary basins exist beneath the West Antarctic interior ice reservoir, till-lubricated ice streams should be able to rapidly drain the ice. If sedimentary basins do not exist beneath the interior ice reservoir, then a mechanism other than sediment-lubricated ice streams may be required to rapidly drain the ice sheet. We conclude that geological structures beneath the

West Antarctic Ice Sheet have the potential to dictate the evolution of the dynamic ice system, modulating the influence of changes in the global climate system.   □

1. Fairbanks, R. G. A 17,000-year glacio-eustatic sea level record: Influence of glacial melting rates on the Younger Dryas event and deep-ocean circulation. *Nature* **342,** 637–642 (1989).
2. MacAyeal, D. R. Irregular oscillations of the West Antarctic ice sheet. *Nature* **359,** 29–35 (1992).
3. MacAyeal, D. R. Binge/purge oscillations of the Laurentide ice sheet is a cause of the north Atlantic's Heinrich events. *Paleoceanography* **8(6),** 775–784 (1993).
4. Alley, R. B. & Whillans, I. M. Changes in the West Antarctic ice sheet. *Science* **254,** 959–963 (1991).
5. Blankenship, D. D. *et al.* Active volcanism beneath the West Antarctic Ice Sheet and implications for ice-sheet stability. *Nature* **361,** 526–529 (1993).

6. Blankenship, D. D., Bentley, C. R., Rooney, S. T. & Alley, R. B. Till beneath ice stream B.1. Properties derived from seismic travel times. *J. Geophys. Res.* **9,** 8903–8911 (1987).
7. Engelhardt, H., Humphrey, N., Kamb, B. & Fahnestock, M. Physical conditions at the base of a fast moving Antarctic ice stream. *Science* **248,** 57–59 (1990).
8. Engelhardt, H. & Kamb, B. Basal hydraulic system of a West Antarctic ice stream: constraints from borehole observations. *J. Glaciol.* **43,** 207–244 (1997).
9. Dalziel, I. W. D. & Elliot, D. G. West Antarctica: problem child of Gondwanaland. *Tectonics* **1,** 3–19 (1982).
10. Behrendt, J. C. *et al.* The West Antarctic Rift System-A Review of Geophysical Investigations 67–112 (Antarctic Res. Ser. 53, Am. Geophys. Union, Washington DC, 1991).
11. Cooper, A. K., Davey, F. J. & Hinz, K. in *Geological Evolution of Antarctica* (eds Thomson, M. R. A., Crame, J. A. & Thomson, J. W.) 285–292 (Cambridge Univ. Press, 1991).
12. Davey, F. J. *The Antarctic Continental Margin: Geology and Geophysics of the Western Ross Sea* 1–16 (Circum-Pacific Council for Energy and Resources, Houston, 1987).
13. Robertson, J. D., Bentley, C. R., Clough, J. W. & Greischar, L. L. in *Antarctic Geoscience* 1083–1090 (IUGS B4, Univ. Wisconsin Press, Madison, Wisconsin, 1982).
14. Rose, K. E. Characteristics of ice flow in Marie Byrd Land, Antarctica. *J. Glaciol.* **24,** 63–74 (1979).
15. Ten Brink, U. S., Bannister, S., Beaudoin, B. C. & Stern, T. A. Geophysical investigations of the tectonic boundary between East and West Antarctica. *Science* **261,** 45–50 (1993).
16. Rooney, S. T., Blankenship, D. D., Bentley, C. R. & Alley, R. B. Till beneath ice stream B.2. Structure and continuity. *J. Geophys. Res.* **9(B9),** 8913–8920 (1987).
17. Retzlaff, R., Lord, N. & Bentley, C. R. Airborne-radar studies: ice streams A, B and C, West Antarctica. *J. Glaciol.* **39(133),** 495–506 (1993).
18. Hodge, S. M. & Doppelhammer, S. Onset of streaming flow of ice streams. *J. Geophys. Res.* **101,** 6669–6677 (1996).
19. Scambos, T. A. & Bindshadler, R. A. Ice flow at the confluence of two ice stream tributaries revealed by sequential satellite imagery. *Ann. Glaciol.* **17,** 177–182 (1993).
20. Bindshadler, R. A. & Vornberger, P. L. AVHRR imagery reveals Antarctic ice dynamics. *Eos* **71,** 741–742 (1990).
21. Anandakrishnan, S., Blankenship, D. D., Alley, R. B. & Stoffa, P. L. Influence of subglacial geology on the position of a West Antarctic ice stream from seismic observations. *Nature* **394,** 62–65 (1998).
22. Shabtaie, S. & Bentley, C. R. Ice-thickness map of the West Antarctic ice streams by radar sounding. *Ann. Glaciol.* **11,** 126–135 (1988).
23. Drewry, D. J. *Antarctica: Glaciological and Geophysical Folio* (Cambridge Univ. Press, 1983).
24. Shabtaie, S. & Bentley, C. R. West Antarctic ice streams draining into the Ross ice shelf: configuration and mass balance. *J. Geophys. Res.* **92(B2),** 1311–1336 (1987).
25. Anandakrishnan, S. & Alley, R. B. Stagnation of ice stream C, West Antarctica by water piracy. *Geophys. Res. Lett.* **24,** 265–268 (1997).
26. Brozena, J. M. *et al.* CASERTZ 91-92: Airborne gravity and surface topography measurements. *Antarc. J. US* **28,** 1–3 (1993).
27. Behrendt, J. C. *et al.* CASERTZ aeromagnetic data reveal late Cenozoic flood basalts in the West Antarctic rift system. *Geology* **22,** 527–530 (1994).

Influence of subglacial geology on the position of a West Antarctic ice stream from seismic observations

S. Anandakrishnan[*]**, D. D. Blankenship**[†]**, R. B. Alley**[*]
& P. L. Stoffa[†]

[*] *Earth System Science Center and Department of Geosciences, Pennsylvania State University, University Park, Pennsylvania 16802, USA*
[†] *Institute for Geophysics, University of Texas–Austin, Austin, Texas 78759, USA*

. . . .

Ice streams drain much of the interior West Antarctic Ice Sheet and buffer the main ice reservoir from oceanic influences[1,2]. The slow-flowing interior feeds the floating Ross Ice Shelf with ice via fast-flowing ice streams[3] that are believed to modulate sea-level change through their control of inland ice storage. Understanding ice-stream behaviour, and predicting the response to climate change[4], requires a better knowledge of the subglacial geology[5,6]. It is known that a thawed ice-bed and high-pressure basal water are necessary, but not sufficient, conditions to cause ice streaming[7,8]. Moreover, it has been hypothesized that a soft sedimentary bed is also required, because of its intrinsic low frictional resistance to flow[9], and owing to its high erodibility so as to generate till that can deform and lubricate ice motion[10,11], or to bury rough features and smooth the bed for sliding. Here we use seismic observations to provide evidence that one margin of the upglacier part of an ice stream is directly above the boundary of a basin with such sedimentary fill. The ice stream is within the basin and the ice outside the basin is slow-flowing. The basin fill presents an order-of-magnitude lower frictional resistance to ice flow than the subglacial material outside the basin. We conclude that the ice stream position is dependent on subglacial geology.

We identify the ice stream margin by the striking increase in flow velocity from ~ 10 m yr^{-1} to over 60 m yr^{-1} over a distance of 4.5 km (between Km 52.5 and Km 57 of Fig. 1; the Km numbers refer to distance in kilometres from the beginning of our line at Km0) that is correlative with flow-bands in satellite imagery[12,13]. The ice flow velocities (Fig. 1b) as well as the surface elevation were determined by repeat GPS (Global Positioning System) surveying with a one-year interval between surveys. A combined reflection and refraction seismic profile along the GPS profile crossed the boundary between the slow-flowing interior ice of the West Antarctic Ice Sheet and the fast-moving ice-stream ice (Fig. 1a). The seismic data were acquired in the 1994–95 austral summer by using a towed snow-streamer with 14 Hz geophones every 25 m from 0 to 10.5 km distance from the source. The shot interval was 300 m and the line was directed east–west with higher shotpoint numbers (SP) to the west.

Common-shot gathers were collected every 300 m along the line, and the times of first arrival for the direct wave t_d and the subglacially refracted wave t_r were picked (Fig. 2 is a representative gather at location SP = Km 51.0). To interpret these data we first formed a model of the ice and subglacial structure beneath the line and then performed a least-squares inversion to determine model
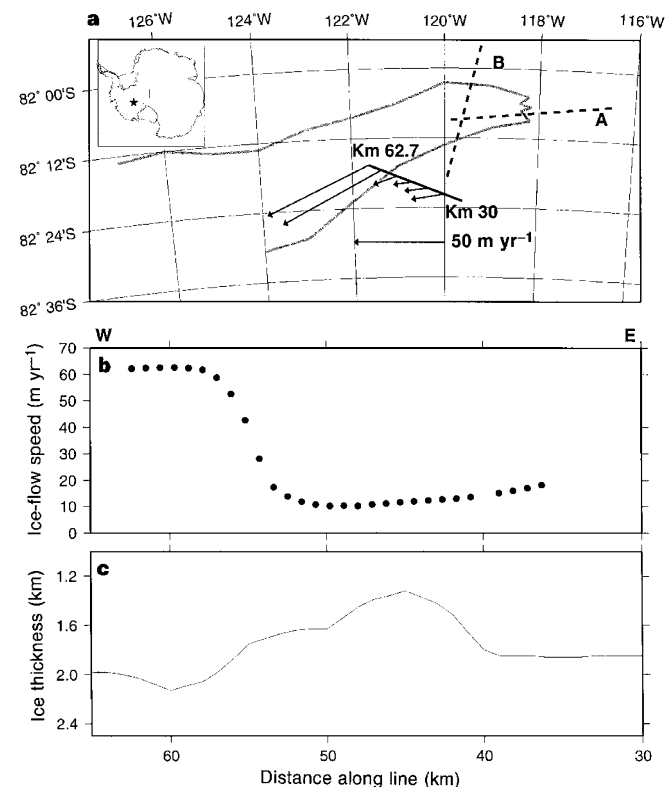

Figure 1 Location map showing the ice stream boundaries and the experiment profile line, together with ice flow speeds and ice thickness along that line. **a**, Map showing the seismic line (solid line) and selected ice flow vectors along the line (determined by repeat GPS measurements; see text). All the measured ice flow speeds are plotted in **b**. The grey curves are the boundaries and onset of ice stream C as identified by Hodge and Doppelhammer[12] (these were digitized from their Fig. 5). The two dashed lines are profiles A and B of Bell *et al.*[13] (included here for reference). The inset is a map of Antarctica with a star marking our study-area. The + symbol indicates the position of the South Pole. **b**, Ice flow speeds (m yr^{-1}); the abscissa is the position along the seismic line in kilometres; **c**, ice thickness in km.